

Chiral 3π -exchange NN-potentials: Results for diagrams proportional to g_A^4 and g_A^6

N. Kaiser

Physik Department T39, Technische Universität München,
D-85747 Garching, Germany

Abstract

We calculate in (two-loop) chiral perturbation theory the local NN-potentials generated by the three-pion exchange diagrams proportional to g_A^4 and g_A^6 . Surprisingly, we find that the total isoscalar central 3π -exchange potential vanishes identically. The individually largest 3π -exchange potentials are of isoscalar spin-spin, isovector central and isoscalar tensor type. For these potentials simple analytical expressions can be given. The strength of these dominant 3π -exchange potentials at $r = 1.0$ fm is 4.6 MeV, 2.9 MeV and 1.4 MeV, respectively. Furthermore, we observe that the spin-spin and tensor potentials due to the diagrams proportional to g_A^6 do not exist in the infinite nucleon mass limit.

PACS: 12.20.Ds, 12.38.Bx, 12.39.Fe, 13.75.Cs.

In a recent work [1] we have started to calculate the static nucleon-nucleon potentials generated by the (two-loop) 3π -exchange diagrams with interaction vertices taken from the leading-order effective chiral πN -Lagrangian. In ref.[1] we restricted ourselves to the evaluation of four relatively simple classes of diagrams which in fact comprise all graphs with the common prefactor g_A^2/f_π^6 . It was stressed in ref.[1] that the chiral $3\pi NN$ -contact vertex depends on the choice of the interpolating pion-field and therefore one has to consider representation invariant classes of diagrams (classes I and II in ref.[1]) by supplementing graphs involving the chiral 4π -vertex. Another obvious consequence of this is that there is no unique way (in chiral perturbation theory) of defining the so-called "pion-nucleon form factor" which is often introduced in phenomenological models. The only meaningful separation of the interaction potential is the one into point-like 1π -exchange and 3π -exchange. The four classes of chiral 3π -exchange diagrams evaluated in ref.[1] gave rise only to isovector spin-spin and tensor potentials. The strength of the resulting coordinate-space potentials was very weak with values of ± 0.1 MeV and less at a internucleon distance of $r = 1.0$ fm. Compared to the chiral 2π -exchange potentials [2, 3] these are negligibly small corrections.

The purpose of this work is complete the calculation of the chiral 3π -exchange NN-potentials and to present results for the diagrams carrying independent prefactors g_A^4/f_π^6 and g_A^6/f_π^6 . We will see that a grouping of these diagrams into five different classes is very useful.

Let us begin with some basic definitions in order to fix our notation. In the static limit and considering only irreducible diagrams the on-shell NN T-matrix takes the following form:

$$\begin{aligned} \mathcal{T}_{NN} = & V_C(q) + V_S(q) \vec{\sigma}_1 \cdot \vec{\sigma}_2 + V_T(q) \vec{\sigma}_1 \cdot \vec{q} \vec{\sigma}_2 \cdot \vec{q} \\ & + \left[W_C(q) + W_S(q) \vec{\sigma}_1 \cdot \vec{\sigma}_2 + W_T(q) \vec{\sigma}_1 \cdot \vec{q} \vec{\sigma}_2 \cdot \vec{q} \right] \vec{\tau}_1 \cdot \vec{\tau}_2, \end{aligned} \quad (1)$$

where $q = |\vec{q}|$ denotes the momentum transfer between the initial and final state nucleon. The subscripts C, S and T refer to the central, spin-spin and tensor components, each of which occurs in an isoscalar (V) and an isovector (W) version. As indicated, the (real) NN-amplitudes $V_C(q), \dots, W_T(q)$ depend only on the momentum transfer q in the static limit. We are here interested only in the coordinate-space potentials generated by certain diagrams in which three pions are simultaneously exchanged between both nucleons. For this purpose it is sufficient to calculate the imaginary parts of the NN-amplitudes $V_{C,S,T}(q)$ and $W_{C,S,T}(q)$ analytically continued to time-like momentum transfer $q = i\mu - 0^+$ with $\mu \geq 3m_\pi$. These imaginary parts are then the mass-spectra entering a representation of the local coordinate space potentials in form of a continuous superposition of Yukawa functions,

$$\tilde{V}_C(r) = -\frac{1}{2\pi^2 r} \int_{3m_\pi}^{\infty} d\mu \mu e^{-\mu r} \text{Im } V_C(i\mu) , \quad (2)$$

$$\tilde{V}_S(r) = \frac{1}{6\pi^2 r} \int_{3m_\pi}^{\infty} d\mu \mu e^{-\mu r} \left[\mu^2 \text{Im } V_T(i\mu) - 3 \text{Im } V_S(i\mu) \right] , \quad (3)$$

$$\tilde{V}_T(r) = \frac{1}{6\pi^2 r^3} \int_{3m_\pi}^{\infty} d\mu \mu e^{-\mu r} (3 + 3\mu r + \mu^2 r^2) \text{Im } V_T(i\mu) . \quad (4)$$

The isoscalar central, spin-spin and tensor potentials, denoted here by $\tilde{V}_{C,S,T}(r)$, are as usual those ones which are accompanied by the operators 1, $\vec{\sigma}_1 \cdot \vec{\sigma}_2$ and $3\vec{\sigma}_1 \cdot \hat{r} \vec{\sigma}_2 \cdot \hat{r} - \vec{\sigma}_1 \cdot \vec{\sigma}_2$, respectively. For the isovector potentials $\tilde{W}_{C,S,T}(r)$ a completely analogous representation holds.

Let us now turn to the evaluation of the NN-potentials from the two-loop 3π -exchange diagrams. Application of the Cutkosky cutting rules gives the relevant imaginary parts $\text{Im } V_{C,S,T}(i\mu)$ and $\text{Im } W_{C,S,T}(i\mu)$ as integrals of the squared $\bar{N}N \rightarrow 3\pi$ transition amplitudes over the Lorentz-invariant three-pion phase space. Some details about these techniques can be found in ref.[4] where the same method has been applied to calculate (two-loop) spectral-functions of nucleon form factors. The pertinent three-body space integrals are most conveniently performed in the three-pion center-of-mass frame. The corresponding on-mass-shell four-momenta of the three pions read in this frame: $k_1^\nu = (\omega_1, \vec{k}_1)$, $k_2^\nu = (\omega_2, \vec{k}_2)$ and $k_3^\nu = (\mu - \omega_1 - \omega_2, -\vec{k}_1 - \vec{k}_2)$. The mass-shell condition $k_3^2 = m_\pi^2$ determines the cosine of the angle between \vec{k}_1 and \vec{k}_2 (called z) as

$$z k_1 k_2 = \omega_1 \omega_2 - \mu(\omega_1 + \omega_2) + \frac{1}{2}(\mu^2 + m_\pi^2) , \quad k_{1,2} = \sqrt{\omega_{1,2}^2 - m_\pi^2} . \quad (5)$$

In the chosen reference frame the four-momenta of the external nucleons can be taken as $P_1^\nu = (\mu/2, p\vec{v})$ and $P_2^\nu = (-\mu/2, p\vec{v})$, where \vec{v} is a (real) unit vector and $p = \sqrt{\mu^2/4 - M^2} = iM + \mathcal{O}(M^{-1})$ in the heavy nucleon limit ($M \rightarrow \infty$). Of course the assignment of P_1^ν and P_2^ν to the external nucleon lines has to be done such that four-momentum conservation holds for the transition $\bar{N}N \rightarrow 3\pi \rightarrow \bar{N}N$. The possible nucleon propagators occurring in diagrams are always of the form

$$\frac{2M}{(P_1 - k_j)^2 - M^2} = \frac{1}{i\vec{v} \cdot \vec{k}_j - \epsilon} , \quad \frac{2M}{(P_2 + k_j)^2 - M^2} = \frac{-1}{i\vec{v} \cdot \vec{k}_j + \epsilon} . \quad (6)$$

The sign of the ϵ -terms in eq.(6) is uniquely fixed from the original relativistic expressions and in the heavy nucleon mass limit ($M \rightarrow \infty$) the positive quantity ϵ becomes infinitesimally small. With these techniques at hand it is possible to perform analytically at least two of the four non-trivial 3π -phase-space integrations [4]. As a check on the heavy nucleon formalism employed we recalculated the imaginary parts of the isoscalar electromagnetic and isovector

axial nucleon form factors and found perfect agreement with the results of ref.[4]. As a further check we applied the methods to calculate the imaginary parts of the 2π -exchange NN-amplitudes. In that case only a much simpler two-body phase space integral needs to be evaluated and one reproduces indeed exactly the results of ref.[2, 3] in a rather short calculation.

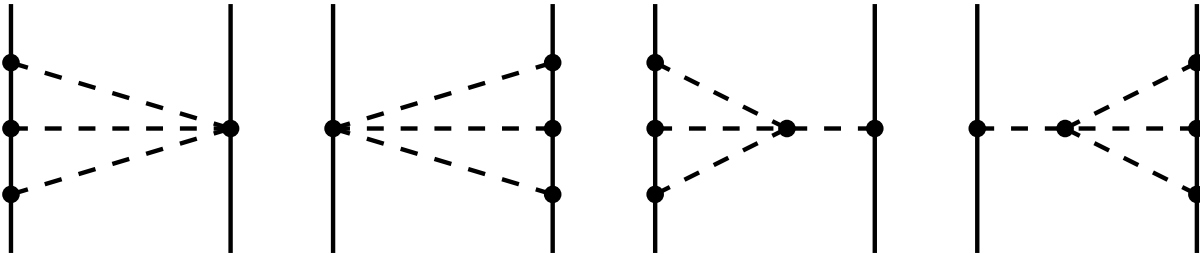


Fig.1: 3π -exchange diagrams of class V proportional to g_A^4 . Solid and dashed lines represent nucleons and pions, respectively.

Let us now turn to the results for the (two-loop) chiral 3π -exchange diagrams proportional to g_A^4 and g_A^6 . We start with the diagrams of class V shown in Fig. 1. As stressed in ref.[1] diagrams involving the chiral $3\pi NN$ -vertex or the chiral 4π -vertex depend on an arbitrary parameter α and therefore one should consider the full class V as one entity. Obviously, the last two pion-pole diagrams in Fig. 1 contribute via coupling constant renormalization also to the point-like 1π -exchange. This effect is however automatically taken care by working with the physical πNN -coupling constant $g_{\pi N}$. From an inspection of the spin- and isospin factors occurring in the diagrams of class V one finds immediately that only non-vanishing isovector spin-spin and tensor NN-amplitudes $W_{S,T}$ will be obtained. We find the following imaginary parts from class V,

$$\text{Im } W_S^{(V)}(i\mu) = \frac{2g_A^4}{3(8\pi f_\pi^2)^3} \iint_{z^2 \leq 1} d\omega_1 d\omega_2 \left\{ k_1^2 + \mu\omega_1 + 3(m_\pi^2 - \mu\omega_1) \left(z + \frac{k_2}{k_1} \right) \frac{\arccos(-z)}{\sqrt{1-z^2}} \right\}, \quad (7)$$

$$\begin{aligned} \text{Im } W_T^{(V)}(i\mu) &= \frac{1}{\mu^2} \text{Im } W_S^{(V)}(i\mu) + \frac{g_A^4 (\mu^2 - m_\pi^2)^{-1}}{\mu^2 (8\pi f_\pi^2)^3} \iint_{z^2 \leq 1} d\omega_1 d\omega_2 \\ &\times \left[(6\mu^2 + 2m_\pi^2)(\omega_1 + \omega_2) - \mu(4\mu^2 + 3m_\pi^2) \right] \\ &\times \left\{ \left[(\mu^2 + m_\pi^2) \left(2\omega_1 - \frac{\mu}{2} \right) - 2\mu\omega_1\omega_2 \right] \frac{\arccos(-z)}{k_1 k_2 \sqrt{1-z^2}} + \mu + 2z\omega_1 \frac{k_2}{k_1} \right\}. \quad (8) \end{aligned}$$

The inequality $z^2 \leq 1$ defines the kinematically allowed (Dalitz) region in the $\omega_1\omega_2$ -plane (which is bounded by a cubic curve) together with the obvious kinematical constraints $m_\pi \leq \omega_{1,2} \leq \mu - 2m_\pi$ and $2m_\pi \leq \omega_1 + \omega_2 \leq \mu - m_\pi$. Note that the same integrand as in eq.(7) for $\text{Im } W_S^{(V)}(i\mu)$ was found in ref.[4] for the spectral-function of the nucleon isovector axial form factor. In the chiral limit $m_\pi = 0$ one can evaluate the remaining double-integrals in eqs.(7,8) using the substitution $\omega_1 = \mu(1 - xy)/2$, $\omega_2 = \mu y/2$ which maps the unit-square $0 \leq x, y \leq 1$ onto the (in the chiral limit) triangle-shaped Dalitz region.

One finds from class V repulsive isovector spin-spin and tensor potentials with an r^{-7} -dependence,

$$\widetilde{W}_S^{(V)}(r)|_{m_\pi=0} = \frac{g_A^4 r^{-7}}{(4\pi)^5 f_\pi^6} \left(\frac{16}{21} \pi^2 + \frac{85}{36} \right), \quad \widetilde{W}_T^{(V)}(r)|_{m_\pi=0} = \frac{g_A^4 r^{-7}}{(4\pi)^5 f_\pi^6} \left(\frac{245}{72} \right). \quad (9)$$

Next, we come to the diagrams of class VI shown in Fig. 2. The isospin factor of the first and second graph is $4\vec{\tau}_1 \cdot \vec{\tau}_2 - 6$ while that of the third and fourth graphs is $-4\vec{\tau}_1 \cdot \vec{\tau}_2 - 6$. The last two graphs are irreducible whereas the first two contain the iteration of 1π -exchange and 2π -exchange (triangle subgraphs). This iterative part has to be separated off in the construction of the NN-potential. A closer inspection reveals that the two types of diagram differ only by some signs in nucleon propagators. The first two diagrams carry a factor $-[(i\vec{v} \cdot \vec{k}_1 + \epsilon)(i\vec{v} \cdot \vec{k}_1 - \epsilon)]^{-1}$ in comparison to a factor $(i\vec{v} \cdot \vec{k}_1 + \epsilon)^{-2}$ from the last two (irreducible) diagrams. The irreducible part of the first two diagrams is obtained by switching the sign of one ϵ -term ($-\epsilon \rightarrow +\epsilon$) such that the expression agrees with that of the irreducible diagrams.

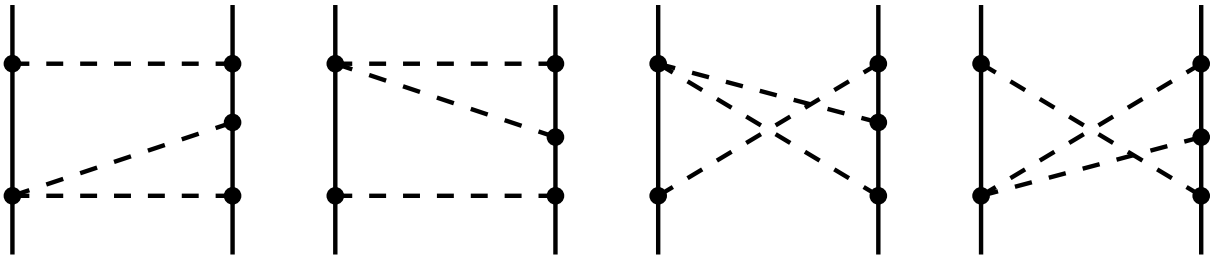


Fig.2: 3π -exchange diagrams of class VI proportional to g_A^4 . Diagrams for which the role of both nucleons is interchanged are not shown. They lead to the same contribution to the NN-potential. The (irreducible) isoscalar NN-amplitudes sum up to zero.

In order to make this procedure more understandable consider the following integrals: $\int_{-1}^1 dx [(x+i\epsilon)(x-i\epsilon)]^{-1} = \pi/\epsilon - 2 + \mathcal{O}(\epsilon^2)$ and $\int_{-1}^1 dx (x+i\epsilon)^{-2} = -2 + \mathcal{O}(\epsilon^2)$. The difference between both diverges as $1/\epsilon$ for $\epsilon \rightarrow 0^+$. According to the definition in eq.(6) one has $\epsilon \sim M^{-1}$ and from the (non-relativistic) Lippmann-Schwinger equation [5] it is known that the iteration of the potential leads to a contribution proportional to the nucleon mass M . Therefore the $1/\epsilon$ -term which gets subtracted by switching the sign (of one ϵ) corresponds indeed to the iterative part. In the case of 2π -exchange all this has been worked out in detail in ref.[2] and as already mentioned the present methods allow to reproduce exactly the results of ref.[2] for the irreducible 2π -exchange.

After subtracting the iterative part the first two and the last two diagrams in Fig. 2 become equal up to a minus-sign. Combining this with the isospin factors one obtains again only a non-vanishing contribution to the isovector spin-spin and tensor NN-amplitudes $W_{S,T}$. We find the following imaginary parts from class VI,

$$\text{Im } W_S^{(VI)}(i\mu) = \frac{2g_A^4}{(8\pi f_\pi^2)^3} \iint_{z^2 \leq 1} d\omega_1 d\omega_2 \left\{ -k_1^2 - \frac{5}{3}\mu\omega_1 + (\mu\omega_1 - m_\pi^2) \left(z + \frac{k_2}{k_1} \right) \frac{\arccos(-z)}{\sqrt{1-z^2}} \right\}, \quad (10)$$

$$\begin{aligned} \text{Im } W_T^{(VI)}(i\mu) &= \frac{1}{\mu^2} \text{Im } W_S^{(VI)}(i\mu) + \frac{2g_A^4}{\mu^2 (8\pi f_\pi^2)^3} \iint_{z^2 \leq 1} d\omega_1 d\omega_2 \omega_1 \left\{ \frac{2\omega_1}{3k_1^2} (2\mu\omega_1 - \mu^2 + 3m_\pi^2 - 6\omega_2^2) \right. \\ &\quad \left. + [(\mu^2 + m_\pi^2)(\mu - 2\omega_1 - 2\omega_2) + 4\mu\omega_1\omega_2] \frac{\arccos(-z)}{k_1 k_2 \sqrt{1-z^2}} - 2z\omega_2 \frac{k_2}{k_1} + 3\omega_1 - 2\mu \right\}. \quad (11) \end{aligned}$$

In the chiral limit ($m_\pi = 0$) one gets now a repulsive isovector spin-spin potential and an attractive isovector tensor potential of the form,

$$\widetilde{W}_S^{(VI)}(r)|_{m_\pi=0} = \frac{g_A^4 r^{-7}}{(4\pi)^5 f_\pi^6} \left(\frac{175}{36} \right), \quad \widetilde{W}_T^{(VI)}(r)|_{m_\pi=0} = \frac{g_A^4 r^{-7}}{(4\pi)^5 f_\pi^6} \left(\frac{4}{3}\pi^2 - \frac{665}{36} \right). \quad (12)$$

Next, we come the diagrams of class VII shown Fig.3. The isospin factor of all four diagrams is 6 and after considering their spin-structure one finds immediately that there will be only a non-vanishing contribution to the isoscalar spin-spin and tensor NN-amplitudes $V_{S,T}$. In the case of class VII one can actually solve all integrals analytically and one obtains the following closed form expressions for the imaginary parts,

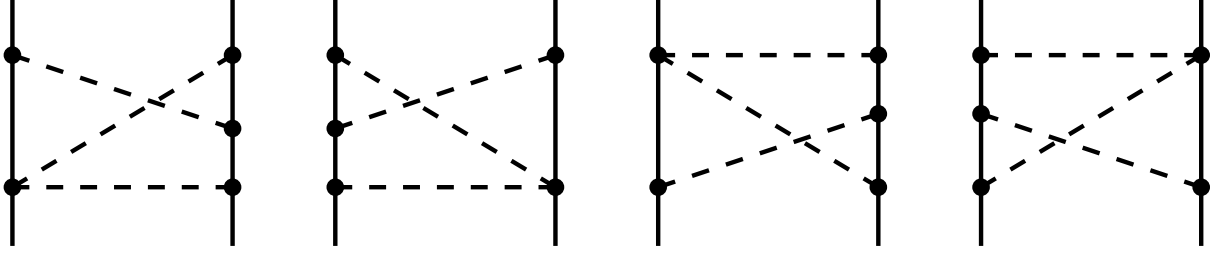


Fig.3: 3π -exchange diagrams of class VII proportional to g_A^4 . The isospin factor of these diagrams is 6.

$$\text{Im } V_S^{(VII)}(i\mu) = \frac{g_A^4(\mu - 3m_\pi)^2}{35\pi(32f_\pi^3)^2} \left[2m_\pi^2 - 12\mu m_\pi - 2\mu^2 + 15\frac{m_\pi^3}{\mu} + 2\frac{m_\pi^4}{\mu^2} + 3\frac{m_\pi^5}{\mu^3} \right], \quad (13)$$

$$\text{Im } V_T^{(VII)}(i\mu) = \frac{g_A^4(\mu - 3m_\pi)}{35\pi(32\mu f_\pi^3)^2} \left[\mu^3 + 3\mu^2 m_\pi + 2\mu m_\pi^2 + 6m_\pi^3 + 18\frac{m_\pi^4}{\mu} - 9\frac{m_\pi^5}{\mu^2} - 27\frac{m_\pi^6}{\mu^3} \right]. \quad (14)$$

It is even more astonishing that the corresponding coordinate space potentials (inserting eqs.(13,14) into eqs.(3,4)) can be expressed through a simple exponential-function multiplied by a polynomial. We find the following repulsive isoscalar spin-spin and tensor potentials from class VII,

$$\tilde{V}_S^{(VII)}(r) = \frac{g_A^4}{2(8\pi f_\pi^2)^3} \frac{e^{-3m_\pi r}}{r^7} (1 + m_\pi r)^2 (2 + m_\pi r)^2, \quad (15)$$

$$\tilde{V}_T^{(VII)}(r) = \frac{g_A^4}{2(8\pi f_\pi^2)^3} \frac{e^{-3m_\pi r}}{r^7} (1 + m_\pi r)^2 (1 + m_\pi r + m_\pi^2 r^2). \quad (16)$$

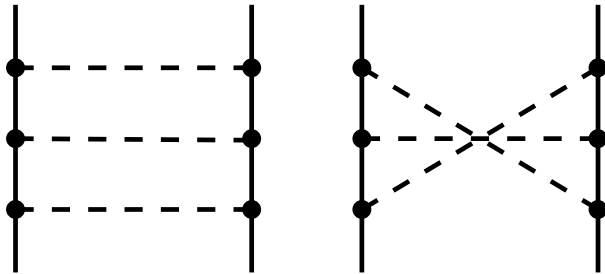


Fig.4: 3π -exchange diagrams of class VIII proportional to g_A^6 .

Next, we consider the diagrams of class VIII shown in Fig.4. The isospin factor of the first graph is $7\vec{\tau}_1 \cdot \vec{\tau}_2 - 6$ while that of the second one is $7\vec{\tau}_1 \cdot \vec{\tau}_2 + 6$. In order to separate off the iterative parts from the first diagram one has to switch the sign of two different ϵ -terms in nucleon propagators. After this procedure the factors coming from the nucleon propagators agree identically for both diagrams in Fig.4. The two diagrams differ however in the ordering of the first and third (spin-dependent) pion-coupling to one nucleon line. Exploiting furthermore the properties of $\vec{\sigma}$ -matrices one finds that the spin-independent part

of this particular 3π -exchange interaction is equal with opposite sign for both diagrams, whereas the spin-dependent part is equal with the same sign. Combining this result with the isospin factors one obtains only non-vanishing isoscalar central (V_C) and isovector spin-spin and tensor ($W_{S,T}$) NN-amplitudes. Explicit evaluation of the diagrams of class VIII leads to the following imaginary part of the isoscalar central NN-amplitude,

$$\text{Im } V_C^{(VIII)}(i\mu) = -\frac{3g_A^6\mu^2}{2(8\pi f_\pi^2)^3} \iint_{z^2 \leq 1} d\omega_1 d\omega_2 \left\{ 1 + \frac{z}{\sqrt{1-z^2}} \arccos(-z) \right\}. \quad (17)$$

In the chiral limit ($m_\pi = 0$) one finds a repulsive isoscalar central potential with an r^{-7} -dependence of the following form,

$$\tilde{V}_C^{(VIII)}(r)|_{m_\pi=0} = \frac{g_A^6 r^{-7}}{(4\pi)^5 f_\pi^6} (60 - 4\pi^2). \quad (18)$$

A similar calculation gives for the imaginary part of the isovector spin-spin NN-amplitude W_S generated by class VIII the following result,

$$\begin{aligned} \text{Im } W_S^{(VIII)}(i\mu) \stackrel{?}{=} & \frac{14g_A^6}{(16\pi f_\pi^2)^3} \iint_{z^2 \leq 1} d\omega_1 d\omega_2 \left\{ \frac{1}{3}(\omega_1^2 - \mu^2 - 4m_\pi^2 + 8\mu\omega_1) \right. \\ & \left. + \left[z + \frac{\arccos(-z)}{\sqrt{1-z^2}} \right] \frac{\mu\omega_1 - m_\pi^2}{k_1(1-z^2)} \left[\frac{z}{k_1}(m_\pi^2 - \mu\omega_1) + \frac{m_\pi^2 - \mu\omega_2}{k_2} \right] \right\}. \quad (19) \end{aligned}$$

However, as indicated by the question mark this results is of no use. On the boundary of the Dalitz region, $z^2 = 1$, the integrand in eq.(19) has singularities of the form $(1-z^2)^{-1}$ and $(1-z^2)^{-3/2}$ such that the double-integral $\iint_{z^2 \leq 1} d\omega_1 d\omega_2$ diverges. The same non-integrable singularities were found in an explicit calculation of $\text{Im } W_T^{(VIII)}(i\mu)$. Therefore one has to conclude that the isovector spin-spin and tensor potentials generated by the diagrams of class VIII do not exist in the infinite nucleon mass ($M \rightarrow \infty$) or static limit. Note that this statement applies separately to the second (irreducible) diagram in Fig. 4 and the occurrence of these singularities has nothing to do with adding the (irreducible components of the) first diagram. Presently, we do not have a detailed understanding of the problem encountered here. Most likely it originates from the fact that several nucleon propagators in the infinite mass limit $M \rightarrow \infty$ can introduce severe singularities in loop-functions as the following one-loop example shows,

$$\int \frac{d^4l}{i(2\pi)^4} \frac{1}{(l_0 - \omega)^3 (m_\pi^2 - l^2)} = \frac{1}{8\pi^2} \left[\frac{\omega}{m_\pi^2 - \omega^2} + \frac{m_\pi^2}{(m_\pi^2 - \omega^2)^{3/2}} \arccos \frac{-\omega}{m_\pi} \right]. \quad (20)$$

The discovery of the non-finiteness of the isovector spin-spin and tensor potentials due to class VIII in the static ($M \rightarrow \infty$) limit points towards a further limitation of the heavy baryon approach when applied to the two-nucleon system. It seems that once the number of heavy nucleon propagators exceeds a critical value the corresponding two-loop integrals do not exist anymore (for $M \rightarrow \infty$). Of course a deeper understanding of this feature would be very desirable.

Finally, we consider the diagrams of class IX shown in Fig. 5. The isospin factor of the first and second diagram is $-6 - \vec{\tau}_1 \cdot \vec{\tau}_2$ while that of the third and fourth diagram is $6 - \vec{\tau}_1 \cdot \vec{\tau}_2$. The iterative parts of the last two diagrams are separated off in the standard way by switching one sign of an ϵ -term in a single nucleon propagator. After a lengthy calculation we find for the imaginary part of the isoscalar central NN-amplitude V_C from class IX,

$$\text{Im } V_C^{(IX)}(i\mu) = \frac{3g_A^6\mu^2}{2(8\pi f_\pi^2)^3} \iint_{z^2 \leq 1} d\omega_1 d\omega_2 \left\{ 1 + \frac{k_2}{k_1\sqrt{1-z^2}} \left[\frac{\pi}{2} - 2 \arccos(-z) \right] \right\}. \quad (21)$$

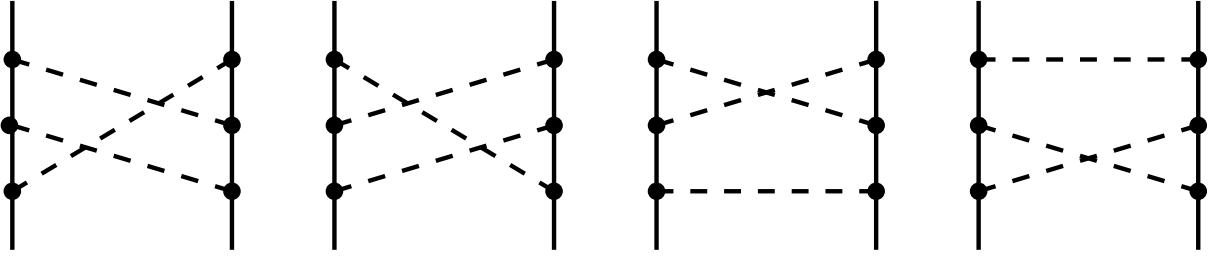


Fig.5: 3π -exchange diagrams of class IX proportional to g_A^6 .

In order to arrive at the very short expression given in eq.(21) we have exploited the inherent permutational symmetry of the 3π -phase space integration. In the chiral limit $m_\pi = 0$ one obtains from class IX an attractive isoscalar central potential of the form

$$\tilde{V}_C^{(IX)}(r)|_{m_\pi=0} = \frac{g_A^6 r^{-7}}{(4\pi)^5 f_\pi^6} (4\pi^2 - 60) , \quad (22)$$

which just cancels the one coming from class VIII given in eq.(18). Later when presenting numerical results in Table 1 we will see that this cancellation holds also for any finite pion mass m_π . Furthermore, we obtain from class IX a non-vanishing contribution to the isovector central NN-amplitude W_C . For the corresponding imaginary part all appearing integrals can be solved analytically and one finds the following closed form expression,

$$\text{Im } W_C^{(IX)}(i\mu) = \frac{g_A^6 (\mu - 3m_\pi)^2}{30\pi\mu(4f_\pi)^6} (3m_\pi^3 + 2\mu m_\pi^2 - 9\mu^2 m_\pi - 4\mu^3) . \quad (23)$$

Inserting this mass-spectrum into eq.(2) one obtains finally a repulsive isovector central potential which can be expressed in terms of a simple exponential-function multiplied by a polynomial,

$$\tilde{W}_C^{(IX)}(r) = \frac{2g_A^6}{(16\pi f_\pi^2)^3} \frac{e^{-3m_\pi r}}{r^7} (1 + m_\pi r)(4 + 5m_\pi r + 3m_\pi^2 r^2) . \quad (24)$$

We have also evaluated the imaginary parts of the isoscalar and isovector spin-spin and tensor NN-amplitudes arising from the four diagrams shown in Fig 5. In these cases there appear again singular terms proportional to $(1-z^2)^{-3/2}$ in the integrands such that the double-integral $\iint_{z^2 \leq 1} d\omega_1 d\omega_2$ diverges. Consequently, we may conclude that only the central potentials generated by the 3π -exchange diagrams proportional to g_A^6 (shown in Figs. 4,5) exist in the static limit ($M \rightarrow \infty$) while all spin-spin and tensor potentials diverge. This is a somewhat unexpected feature of the 3π -exchange NN-potential.

In Table 1, we present numerical results for the coordinate space NN-potentials generated by the 3π -exchange graphs of class V, VI, VII, VIII and IX for internucleon distances $0.6 \text{ fm} \leq r \leq 1.4 \text{ fm}$. We use the parameters $f_\pi = 92.4 \text{ MeV}$, $m_\pi = 138 \text{ MeV}$ (average pion mass) and $g_A = g_{\pi N} f_\pi / M = 1.32$ employing the Goldberger-Treiman relation together with $g_{\pi N} = 13.4$. The choice $g_A = 1.32$ is most natural in the present context since the pion-nucleon coupling is the relevant here and not the axial-vector coupling. One observes that the isovector spin-spin and tensor potentials from classes V and VI (scaling with g_A^4) are a factor 3 to 10 larger than the (largest) potential $\tilde{W}_{S,T}^{(III)}(r)$ found in our previous work [1] on the chiral 3π -exchange diagrams scaling with g_A^2 . The most striking result is that the isoscalar central potentials from class VIII and IX cancel each other, $\tilde{V}_C^{(VIII)}(r) + \tilde{V}_C^{(IX)}(r) = 0$, and this cancellation is found to happen with high numerical precision. From the double-integral representation in eqs.(17,21) it is not at all obvious that the relation $\text{Im } V_C^{(VIII)}(i\mu) + \text{Im } V_C^{(IX)}(i\mu) = 0$ holds, at least we have not yet found a simple analytical proof. Consequently, we can conclude that the

total isoscalar central potential generated by chiral 3π -exchange vanishes identically. Only the exchange of an explicit $\omega(782)$ -vector meson (a strongly resonant 3π -state) can contribute to the (phenomenologically needed) isoscalar central repulsion.

By inspection of Table 1 we furthermore observe that the largest chiral 3π -exchange potentials are the repulsive isoscalar spin-spin and tensor potentials $\tilde{V}_{S,T}^{(VII)}(r)$ due to class VII and the repulsive isovector central potential $\tilde{W}_C^{(IX)}(r)$ due to class IX. These are just the cases in which simple analytical expressions could be given in eqs.(15,16,24). Actually, we are disproving here the claim of ref.[6] that a particular diagram of class I (namely the first graph in Fig. 1 of ref.[1]) would be dominant. Presumably, the strength of the potentials $\tilde{V}_{S,T}^{(VII)}(r)$ and $\tilde{W}_C^{(IX)}(r)$ is still too weak to be of practical relevance. Of course, in order to confirm this an empirical analysis of the low-energy NN-data base as done in ref.[7] including these dominant chiral 3π -exchange potentials would be very desirable.

In summary, we have completed in this work the calculation of the static chiral 3π -exchange NN-potentials by evaluating all diagrams proportional to g_A^4 and g_A^6 . As a surprise we find that the total isoscalar central potential vanishes identically. The individually largest chiral 3π -exchange NN-potentials are of isoscalar spin-spin, isovector central and isoscalar tensor type and for these potentials very simple analytical expressions could be given. We furthermore discovered that the spin-spin and tensor potentials due to class VIII and IX (consisting of diagrams proportional to g_A^6) do not exist in the heavy nucleon mass limit $M \rightarrow \infty$.

r [fm]	0.6	0.7	0.8	0.9	1.0	1.1	1.2	1.3	1.4
$\tilde{W}_S^{(V)}$ [MeV]	51.7	16.5	6.02	2.43	1.06	0.503	0.249	0.129	0.069
$\tilde{W}_T^{(V)}$ [MeV]	16.0	4.99	1.79	0.704	0.302	0.141	0.068	0.035	0.018
$\tilde{W}_S^{(VI)}$ [MeV]	19.9	5.99	2.06	0.783	0.322	0.141	0.065	0.031	0.015
$\tilde{W}_T^{(VI)}$ [MeV]	-30.2	-9.78	-3.63	-1.52	-0.689	-0.326	-0.165	-0.087	-0.048
$\tilde{V}_S^{(VII)}$ [MeV]	214.23	68.81	25.38	10.40	4.62	2.19	1.10	0.575	0.313
$\tilde{V}_T^{(VII)}$ [MeV]	58.39	19.20	7.25	3.05	1.39	0.675	0.347	0.186	0.104
$\tilde{V}_C^{(VIII)}$ [MeV]	177.6	56.2	20.4	8.21	3.58	1.68	0.830	0.429	0.229
$\tilde{V}_C^{(IX)}$ [MeV]	-177.6	-56.2	-20.4	-8.21	-3.58	-1.68	-0.830	-0.429	-0.229
$\tilde{W}_C^{(IX)}$ [MeV]	148.80	46.54	16.75	6.70	2.91	1.36	0.665	0.342	0.183

Tab.1: Numerical values of the local NN-potentials generated by the chiral 3π -exchange graphs of classes V, VI, VII, VIII, IX (shown in Figs. 1, 2, 3, 4, 5) versus the nucleon distance r . The units of these potentials are MeV.

References

- [1] N. Kaiser, *Phys. Rev.* **C61** 0140xx (2000) in print; nucl-th/9910044.
- [2] N. Kaiser, R. Brockmann and W. Weise, *Nucl. Phys.* **A625**, 758 (1997) and refs. therein.
- [3] N. Kaiser, S. Gerstendörfer and W. Weise, *Nucl. Phys.* **A637**, 395 (1998).
- [4] V. Bernard, N. Kaiser and U.G. Meißner, *Nucl. Phys.* **A611**, 429 (1996).
- [5] T. Ericson and W. Weise, *Pions in Nuclei* (Clarendon Press, Oxford, 1988), app. 10.
- [6] J.C. Pupin and M.R. Robilotta, *Phys. Rev.* **C60**, 014003 (1999).
- [7] M.C.M. Rentmeester, R.G.E. Timmermans, J.L. Friar and J.J. de Swart, *Phys. Rev. Lett.* **82**, 4992 (1999).